
Modelling and Forecasting Facility internal report

# Numerical experiments with artificial pressure-wave forcings for ROMS. A sensitivity analysis.

Matjaz Licer

April 29, 2016 [updated June 7, 2016]

## Contents

# 1 Code description and basic equations

This document describes the codes that were used to generate an artificial monochromatic pressure wave NetCDF forcing files for ROMS to evaluate ROMS response at the Mallorca shelf during controled atmospheric conditions. Usual ROMS forcing files are created using `create_WRF_frc_for_ROMS.m` and this is the code I modified to generate forcing NetCDFs containing artificial pressure fields for numerical experiments.

The master code is the `create_WRF_frc_for_ROMS_numExp.m` which is modified in the following ways:

1. a call to the pressure wave generating function `generateArtificialPressureField.m` is added.
2. the pressure wave is written to the NetCDF instead of the `MSLP` air pressure from WRF.
3. the `'bestfit'` option has been disabled.
4. the NetCDF file generation had to be written anew using Matlab intrinsic NetCDF libraries.

As noted, the code `generateArtificialPressureField.m` generates an artificial pressure wave array to be used as ROMS forcing. Its input parameters are pressure wave (group or) phase velocity $c_f$ [km/h], incident angle $\theta$ at which the wave travels across Ciutadella [°] and pressure wave frequency $\nu_W$ [$s^{-1}$]. The angle $\theta$ must be given in nautical (compass) notation ($\theta = 0°$: wave travels north, $\theta = 45°$: wave travels northeast, $\theta = 90°$: wave travels east, $\theta = 120°$: wave travels southeast), see also Figure 1.

The wave pressure wavelength is then computed from $\lambda_W = c_f/\nu_W$ and it angular frequency is $\omega_W = 2\pi\nu_W$. The wave-vector is computed as

$$\vec{k} = \frac{2\pi}{\lambda_W/R_\oplus}[\cos\theta, \sin\theta] \tag{1}$$

where $R_\oplus$ is the Earth radius. Effectively pressure wave wavelength is thus normalized to an arc length in radians using Earth radius. The pressure wave, traveling over Earth surface, is then generated with

$$p(\vec{r}, t) = \left[p_0 + \frac{p_0}{t_R - 1}(t - t_R)\right] \cos(\vec{k} \cdot \vec{r} - \omega t) \tag{2}$$

where $p_0$ is the pressure wave amplitude (set to 1 hPa), $t_R$ is the time ramp during which the wave attains maximum intensity, and $\vec{r} = [\lambda, \phi]$ is the geo-referrenced location (in radians) at the Earth surface. The first square bracket in the formula above is nothing but a linear increase in pressure wave intensity in $t_R$ timesteps.

The pressure wave is then cropped in space to have a lateral width of 1 degree and is oriented along the wave vector axis of propagation $\alpha_P(\theta, \lambda)$, which is computed as

$$\alpha_P(\theta, \lambda) = \tan(\pi/2 - \theta) \cdot (\lambda - \lambda_C) + \phi_C \tag{3}$$

where $\lambda_C$ and $\phi_C$ denote Ciutadella longitude and latitude respectively. The pressure wave is further cropped along its axis. The wave-packet front $\varphi_{WP}(\vec{r},t)$ is defined by the function

$$\varphi_{WP}(\vec{r},t) = \frac{1}{\tan(\pi/2-\theta)} \cdot \left[\lambda_{min} + \frac{c_f \cdot (t-t_0)}{R_\oplus} \cdot \sin\theta + \phi_{min} + \frac{c_f \cdot (t-t_0)}{R_\oplus} \cdot \cos\theta\right] \quad (4)$$

while the wave-packet tail $\tau_{WP}(\vec{r},t)$ is merely a wave-front, time-lagged by the wave duration $\delta t$:

$$\tau_{WP}(\vec{r},t) = \varphi_{WP}(\vec{r},t-\delta t) = \quad (5)$$
$$= \frac{1}{\tan(\pi/2-\theta)} \cdot \left[\lambda_{min} + \frac{c_f \cdot (t-t_0-\delta t)}{R_\oplus} \cdot \sin\theta + \phi_{min} + \frac{c_f \cdot (t-t_0-\delta t)}{R_\oplus} \cdot \cos\theta\right]$$

In the above equations $(\lambda_{min}, \phi_{min})$ denotes the lower left corner of the domain, while $\lambda$ denotes a longitude of each georeferenced point. In this way, pressure wave packets can be generated as coming from arbitrary direction and with arbitrary speed and duration. Example for direction $\theta = 30°$ is depicted in the Figure below.

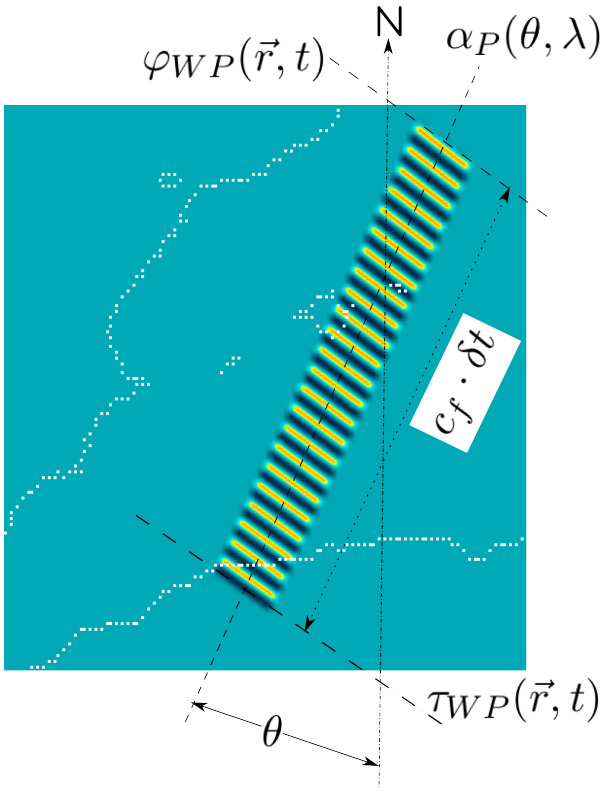


FIGURE 1: Pressure wave packets arriving over Menorca from direction $\theta = 30°$. Axis of propagation $\alpha_P(\theta,\lambda)$, wave-packet front $\varphi_{WP}(\vec{r},t)$ and wave-packet tail $\tau_{WP}(\vec{r},t)$ are also depicted.

## 2 Sensitivity analysis for $\theta$ and $c_f$.

Pressure fields were generated for the following values of parameters:

- $\theta = [0, 10, 20, 30, 40, 50, 60, 70, 80, 90]^\circ$ degrees from north.
- $c_f = [25, 26, 27, 28, 29, 30, 31, 32, 33, 34, 35]$ m/s.
- pressure wave amplitude $p_0 = 3$ hPa.
- pressure wave frequency $10^{-3}$ s$^{-1}$.

ROMS model was run for all these values of parameters using the artificial pressure forcing files generated from the above parameters. SSH from ROMS output files were then extracted along several locations on the 75 m isobath around Mallorca and Menorca, as depicted in Figure 2. Extracting points along the isobath minimizes the effects of topographic amplification. Stations `Off Ciutadella` and `Ciutadella` are the only ones that do not lie along the isobath. The `Ciutadella` point was taken from the ROMS child model, while all the others were extracted from ROMS parent model.

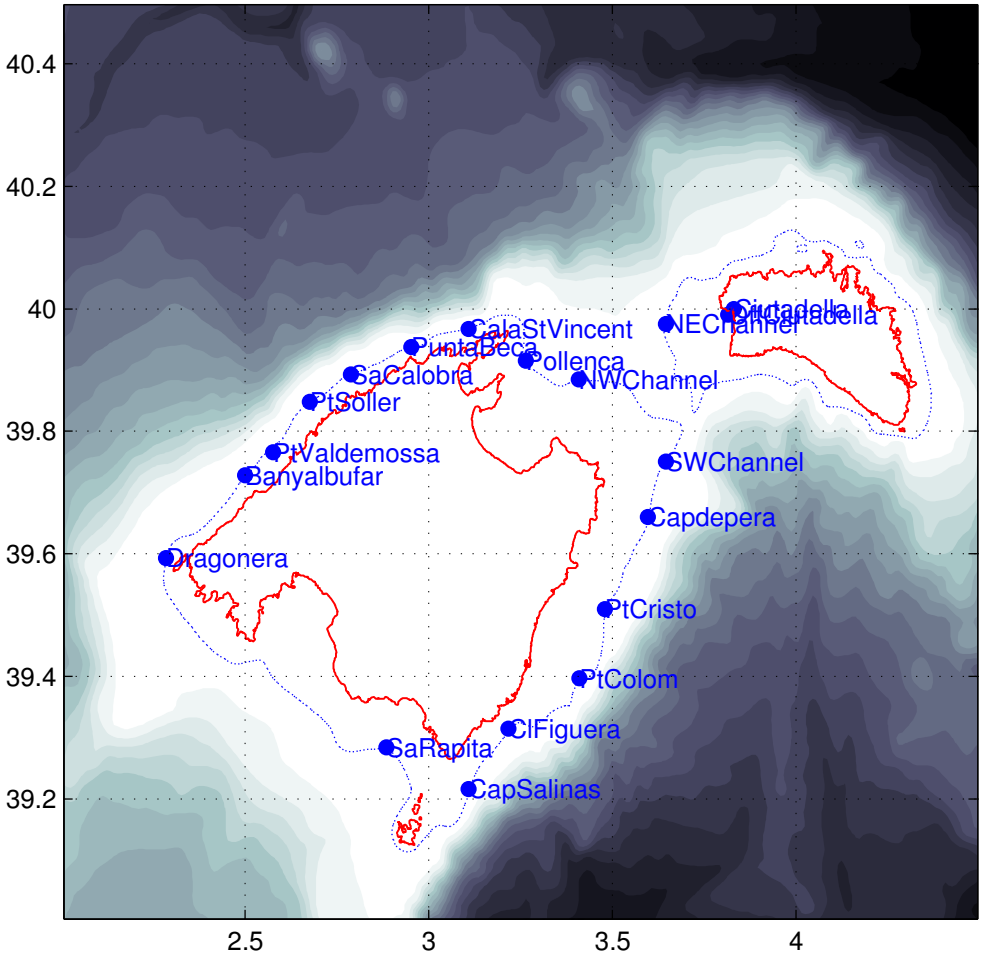


FIGURE 2: Extracted locations along the 75 m isobath around Mallorca and Menorca.

Maximum SSH elevation was then extracted relative to the pressure disturbance phase speed and incident angle at each of these locations and matrices of values thus-obtained are presented on the following pages inFigures 3 - 9. Each of the depicts maximum elevation developed in ROMS, depending on the angle and the phase speed of the pressure disturbance.

There are several things to be noticed about these results. Capdepera, for example, is on the northern end of the Mallorcan shelf and we expect the Proudman resonance effect to be most pronounced there. In the case of Proudman resonance one would expect the amplitude of the SSH anomaly to rise from south-west to north-east along the eastern Mallorcan shelf between Cabo Salinas and Capdepera. In the case of coastal trapped waves these would not necessarily be the case. If we take a look at the Figures 10 - 19 we notice that SSH anomalies exhibit maximum growth between Cabo Salinas to Capdepera (from south-west to north-east) in the case where $\theta = 30°$ and $c_f \geq 33$ m/s. Taking a look at Capdepera matrix on Figure 7 we notice that maximum elevations occur if the incident propagation angle is $\theta = 30$ degrees and $c_f = 33$ m/s. Maximum elevation at the Off Ciutadella point occurs roughly at angles $\theta = 40 - 50$ degrees and $c_f = 33 - 34$ m/s. Most importanly, maximum SSH variability at the Ciutadella harbour occurs if $\theta = 40 - 50$ degrees and $c_f = 30 - 32$ m/s - at these cases the Off Ciutadella SSH is not maximum. In other words: maximum elevations *at the opening of* the Ciutadella harbour do not in themselves imply maximum elevations *in* the Ciutadella harbour.

Furthermore, we checked the maximum SSH variability at different locations along the east Mallorca shelf to see if maximum SSH rises as the wave travels north, as would be expected from the Proudman resonance. These results are depicted in Figures 10 - 19.

If we take a look at the SSH maps (not shown) two SSH anomaly inducing mechanisms stemming from an atmospheric pressure wave are clearly visible:

- the inverse barometric response, amplified by the **Proudman resonance**
- **coastal trapped waves**, traveling around Mallorca and Menorca during and after the passing of the pressure wave. (see also http://digital.csic.es/bitstream/10261/98916/1/Liu-GRL-2002-v29-n17-p28-1.pdf)

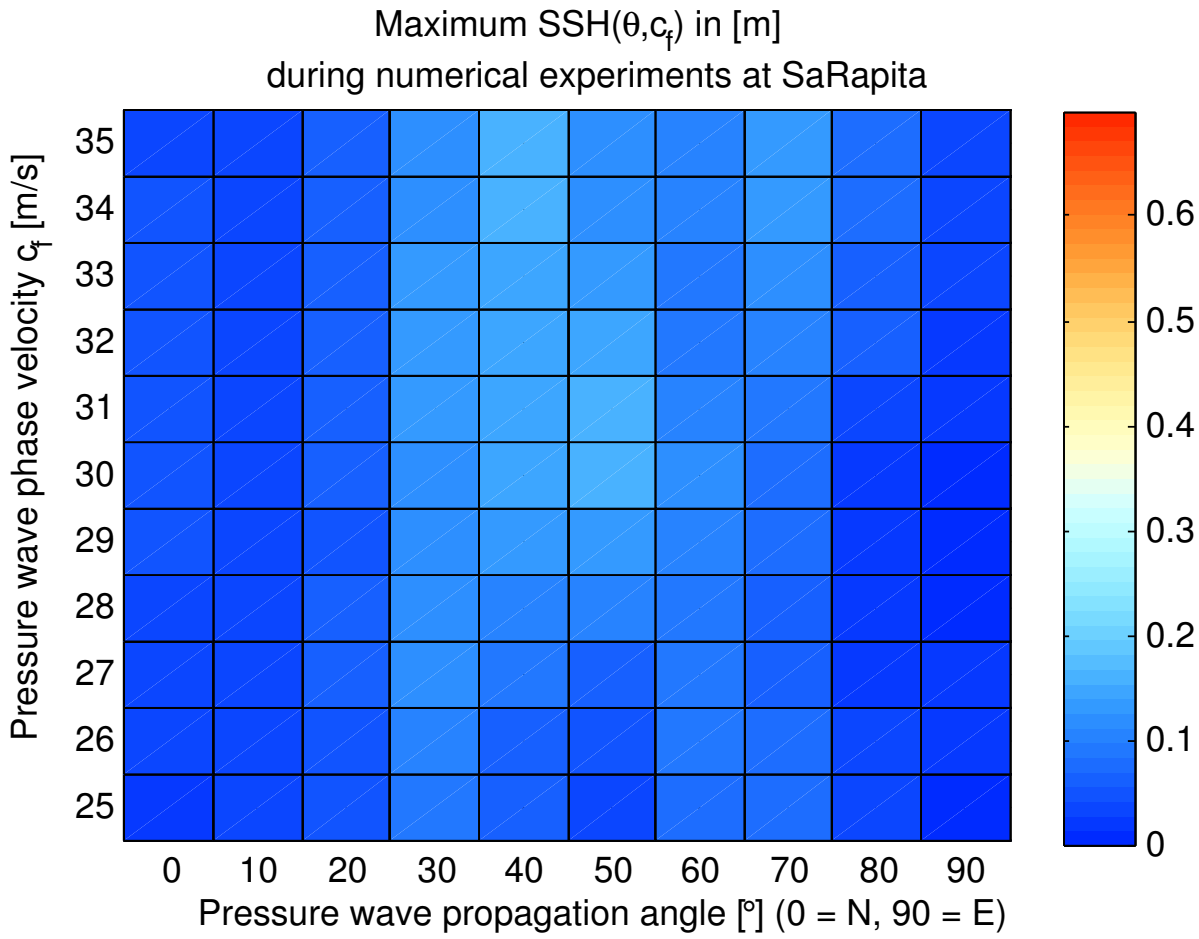


FIGURE 3: Maximum elevation developed in ROMS, depending on the angle and the phase speed of the pressure disturbance.

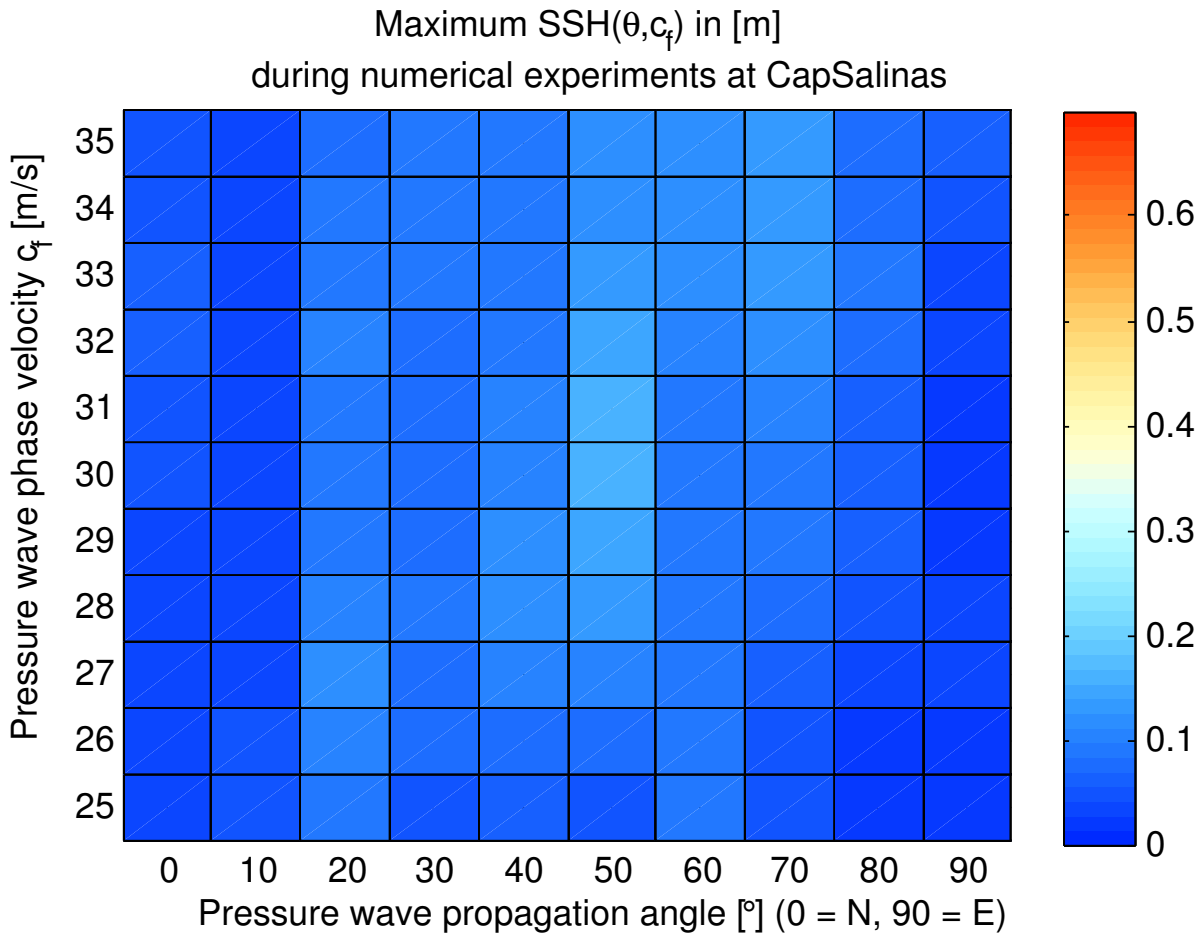


FIGURE 4: Maximum elevation developed in ROMS, depending on the angle and the phase speed of the pressure disturbance.

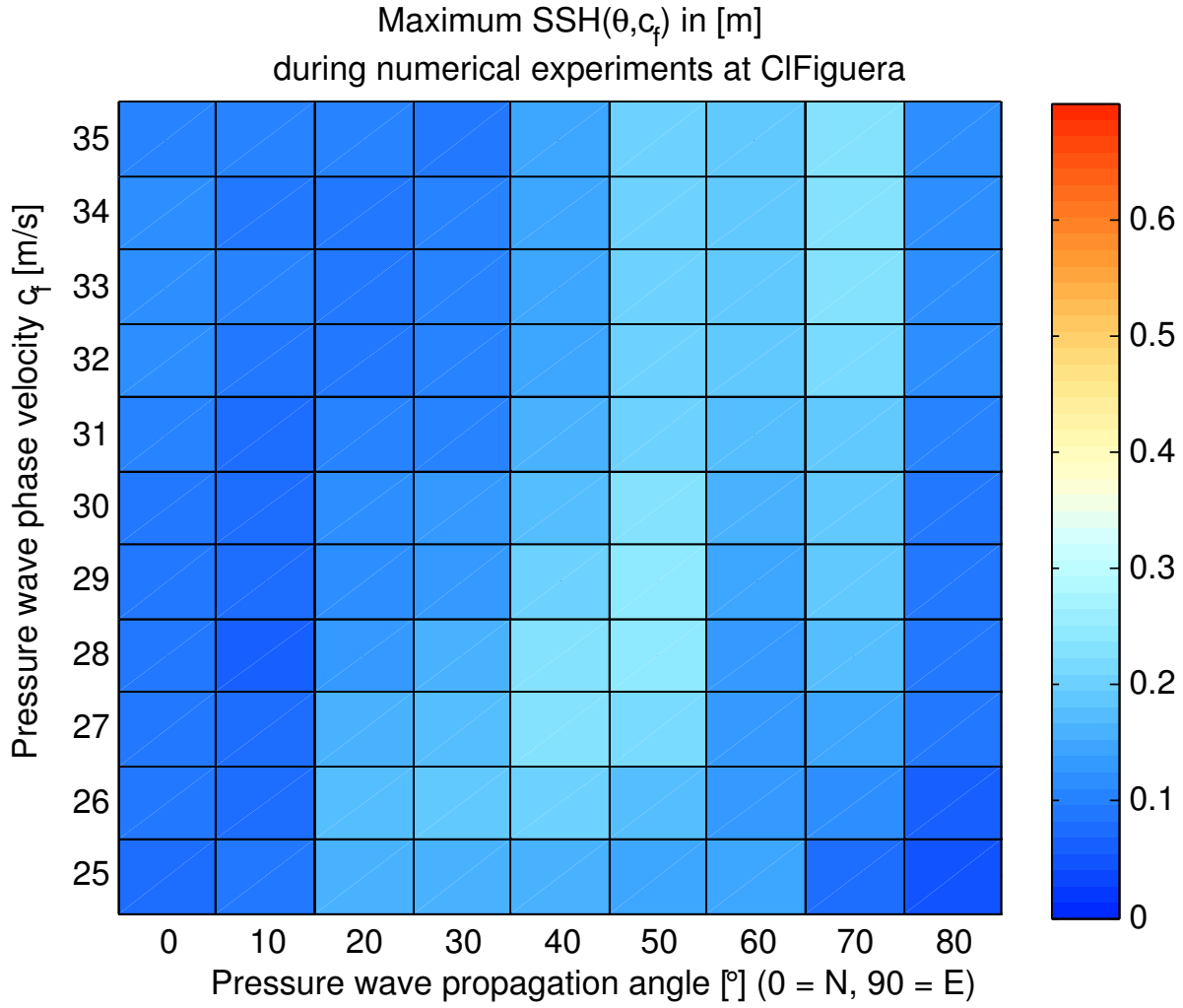


FIGURE 5: Maximum elevation developed in ROMS, depending on the angle and the phase speed of the pressure disturbance.

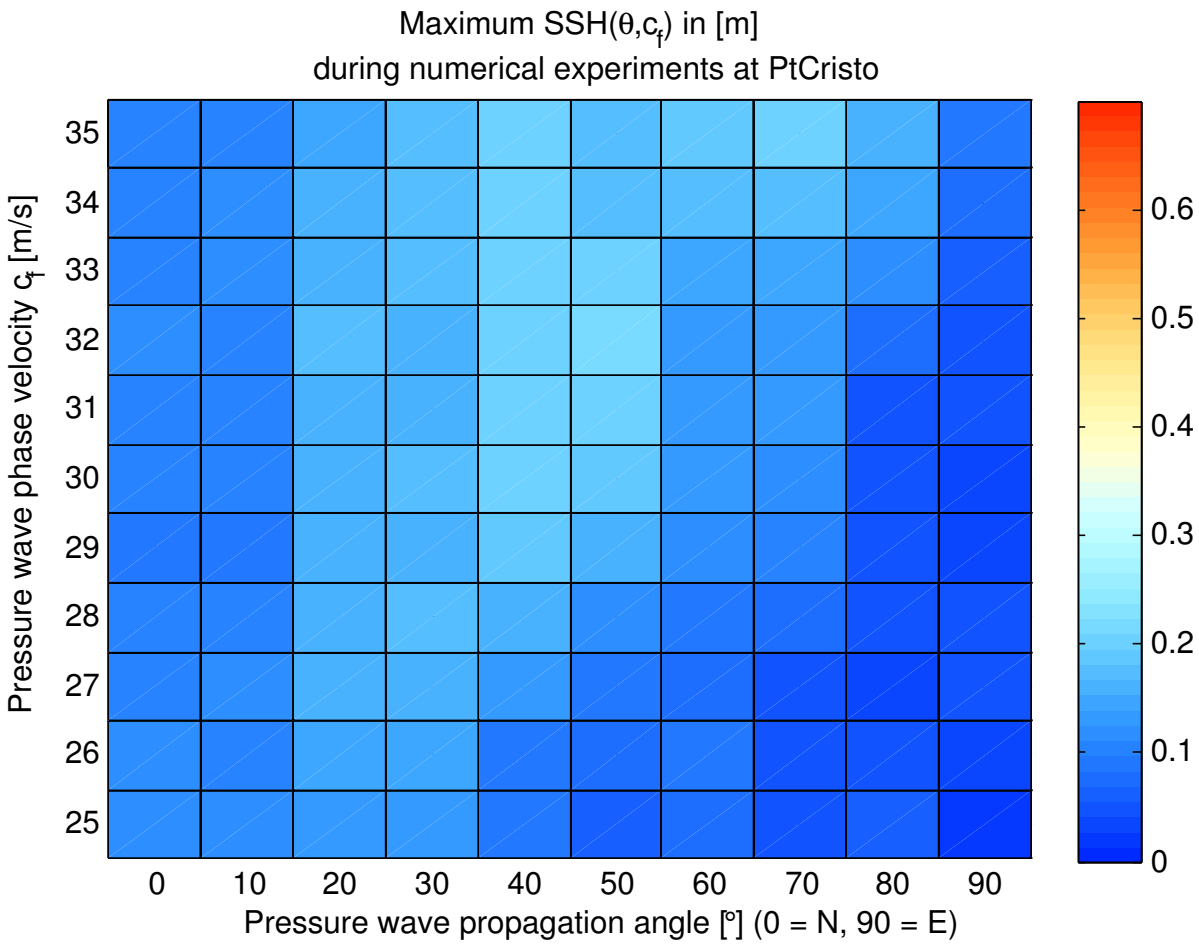


FIGURE 6: Maximum elevation developed in ROMS, depending on the angle and the phase speed of the pressure disturbance.

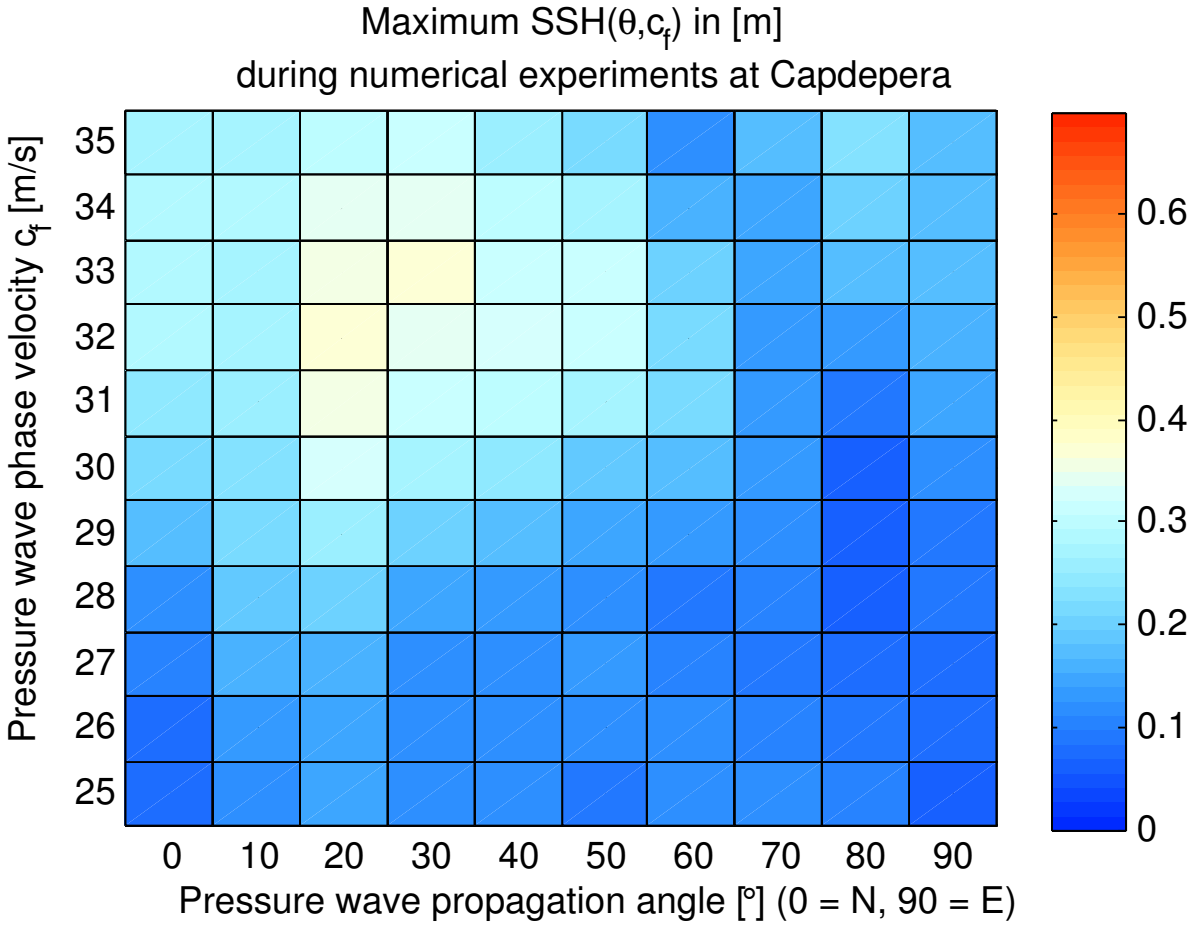


FIGURE 7: Maximum elevation developed in ROMS, depending on the angle and the phase speed of the pressure disturbance.

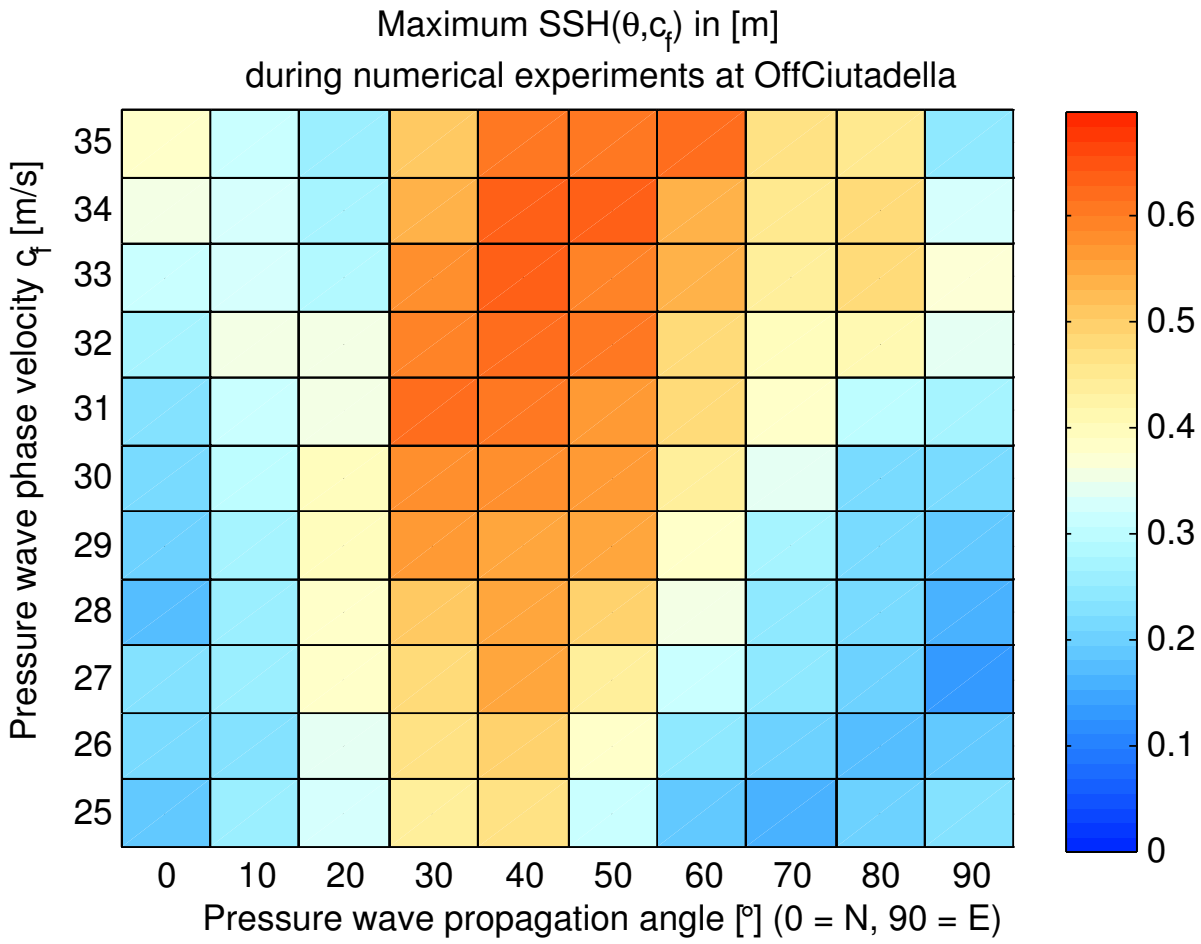


FIGURE 8: Maximum elevation developed in ROMS, depending on the angle and the phase speed of the pressure disturbance.

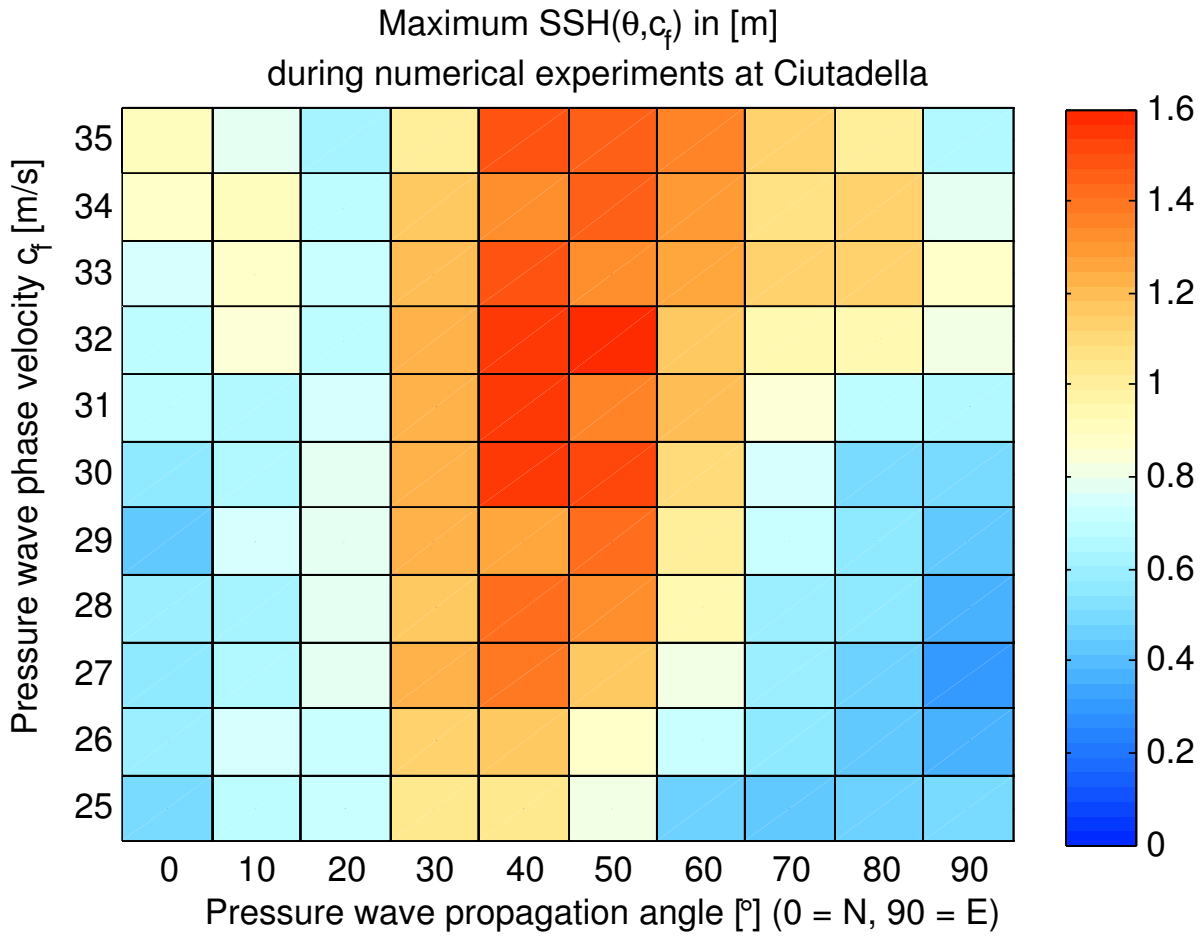


FIGURE 9: Maximum elevation developed in ROMS, depending on the angle and the phase speed of the pressure disturbance.

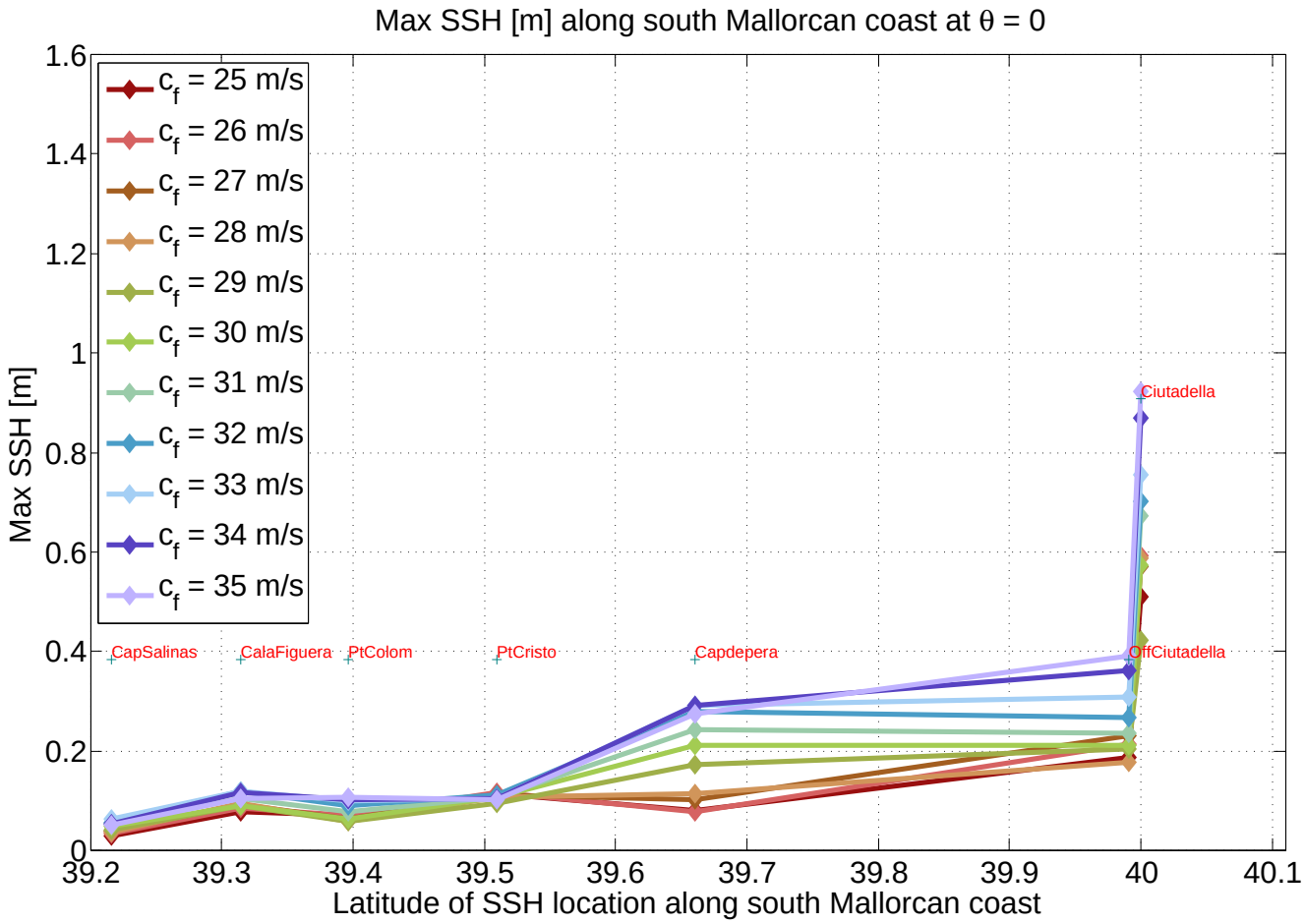


FIGURE 10: Maximum elevation developed along the east Mallorca shelf, depending on the the phase speed of the pressure disturbance and on the sampling location. The names of locations (red letters) are inserted at their respective latitudes for orientation.

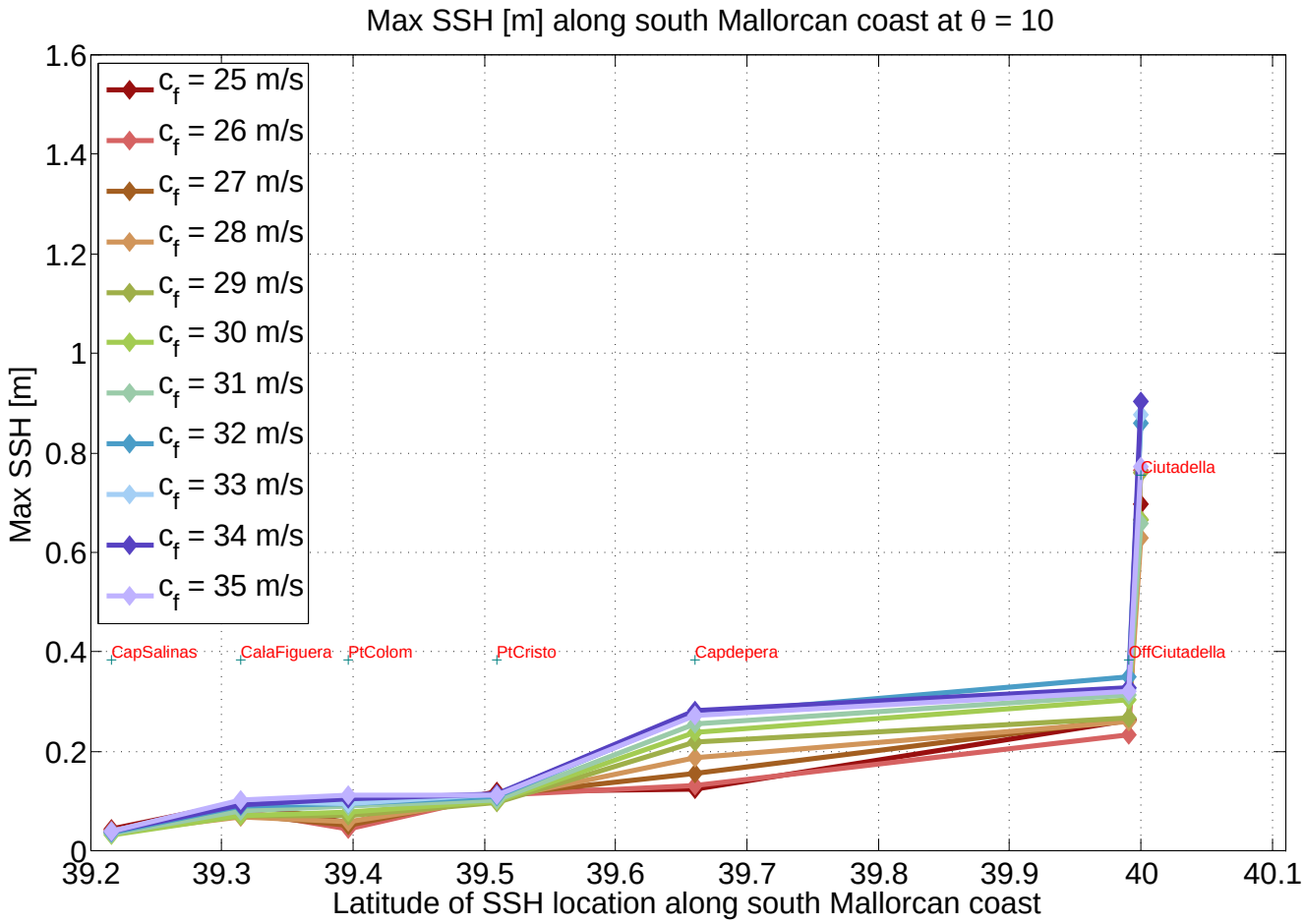


FIGURE 11: Maximum elevation developed along the east Mallorca shelf, depending on the the phase speed of the pressure disturbance and on the sampling location. The names of locations (red letters) are inserted at their respective latitudes for orientation.

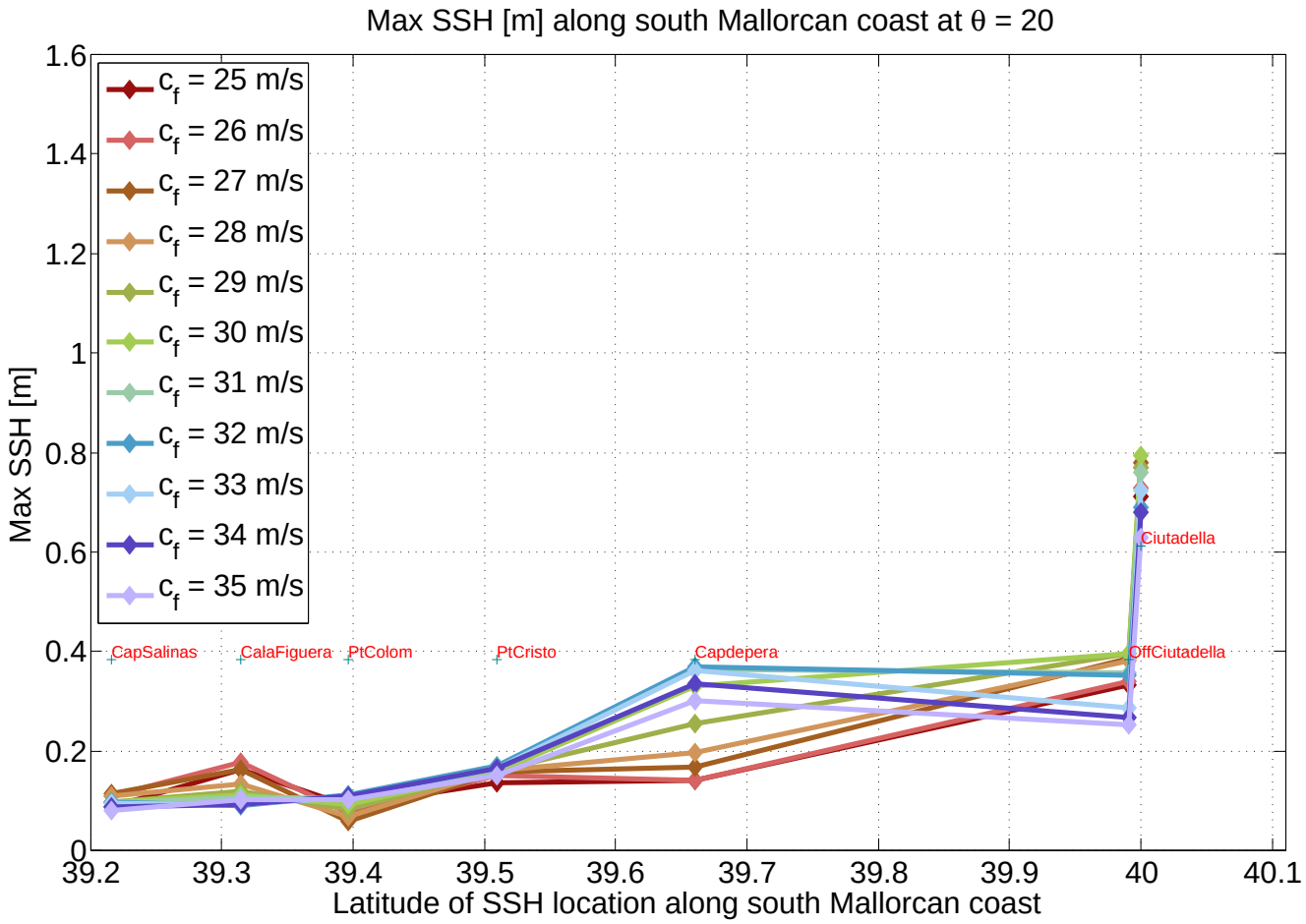


FIGURE 12: Maximum elevation developed along the east Mallorca shelf, depending on the the phase speed of the pressure disturbance and on the sampling location. The names of locations (red letters) are inserted at their respective latitudes for orientation.

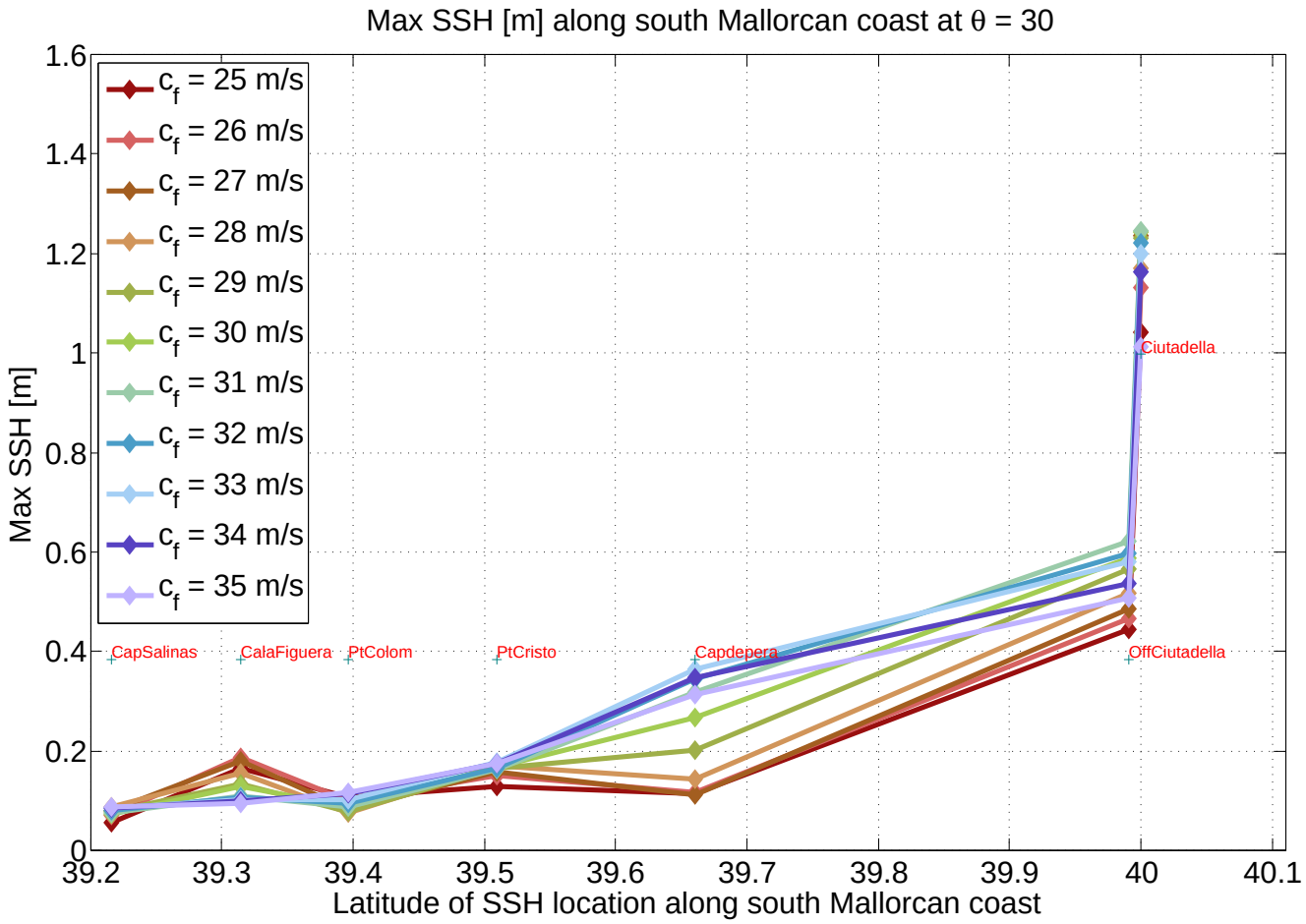


FIGURE 13: Maximum elevation developed along the east Mallorca shelf, depending on the the phase speed of the pressure disturbance and on the sampling location. The names of locations (red letters) are inserted at their respective latitudes for orientation.

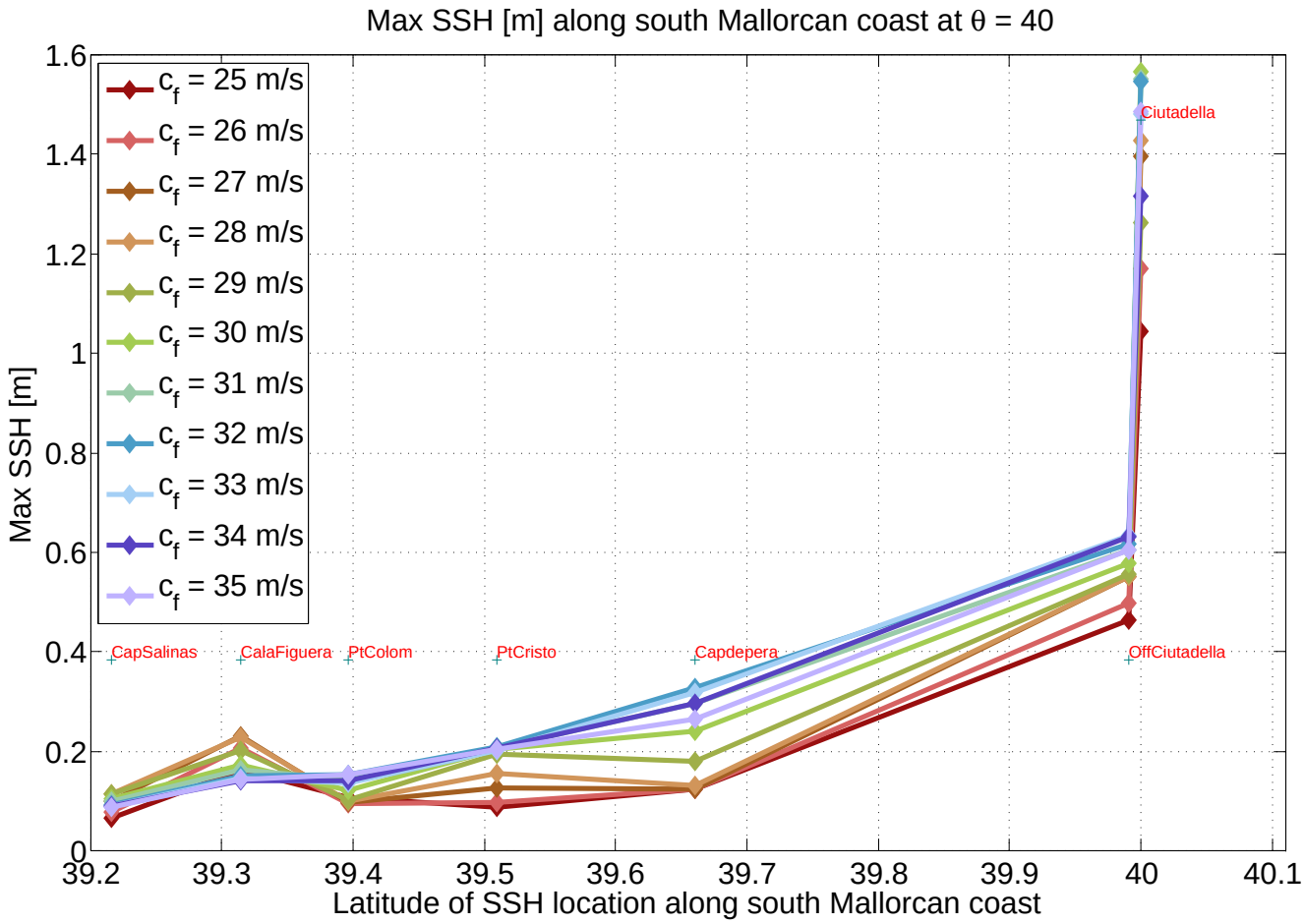


FIGURE 14: Maximum elevation developed along the east Mallorca shelf, depending on the the phase speed of the pressure disturbance and on the sampling location. The names of locations (red letters) are inserted at their respective latitudes for orientation.

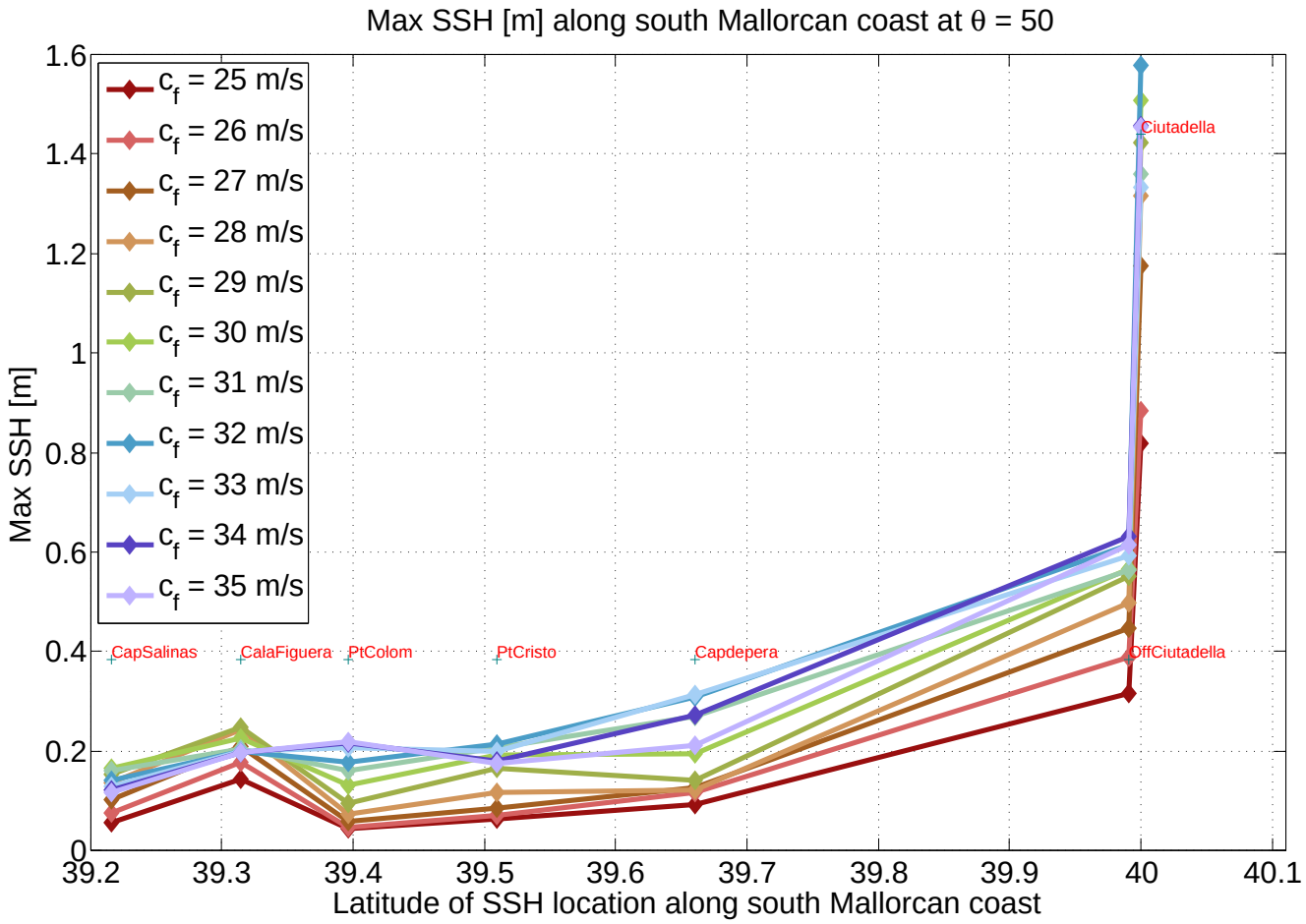


FIGURE 15: Maximum elevation developed along the east Mallorca shelf, depending on the the phase speed of the pressure disturbance and on the sampling location. The names of locations (red letters) are inserted at their respective latitudes for orientation.

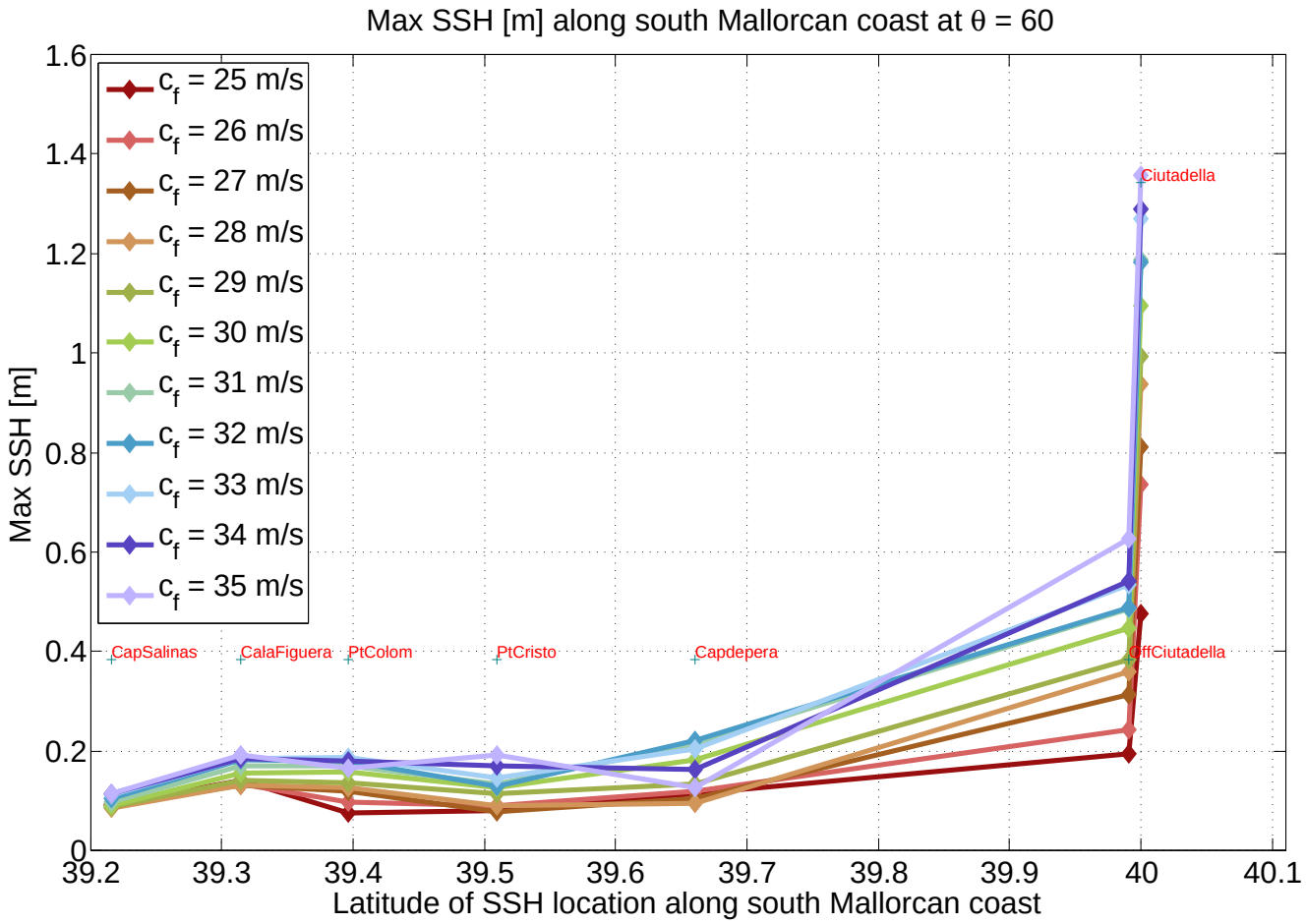


FIGURE 16: Maximum elevation developed along the east Mallorca shelf, depending on the the phase speed of the pressure disturbance and on the sampling location. The names of locations (red letters) are inserted at their respective latitudes for orientation.

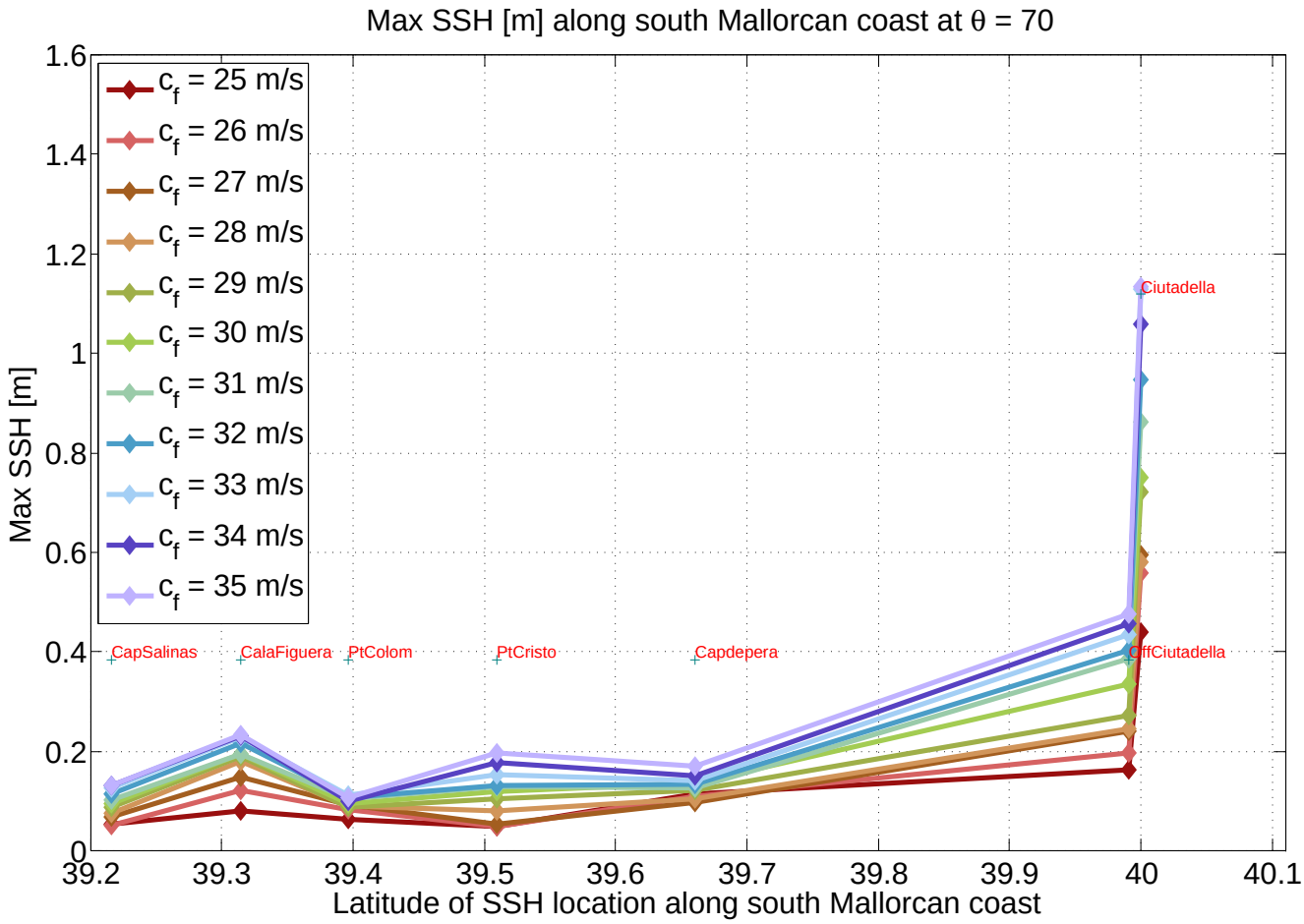


FIGURE 17: Maximum elevation developed along the east Mallorca shelf, depending on the the phase speed of the pressure disturbance and on the sampling location. The names of locations (red letters) are inserted at their respective latitudes for orientation.

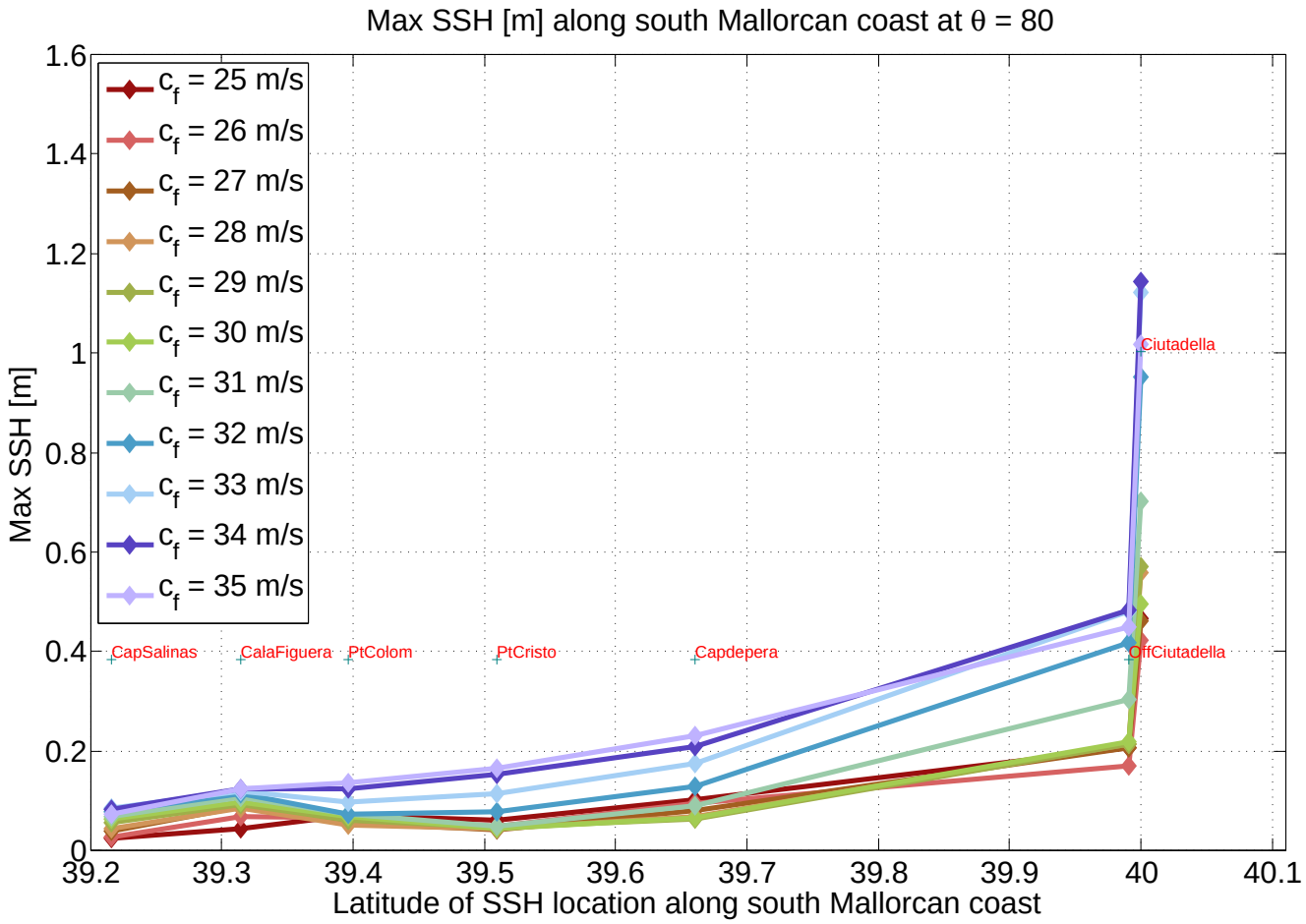


FIGURE 18: Maximum elevation developed along the east Mallorca shelf, depending on the the phase speed of the pressure disturbance and on the sampling location. The names of locations (red letters) are inserted at their respective latitudes for orientation.

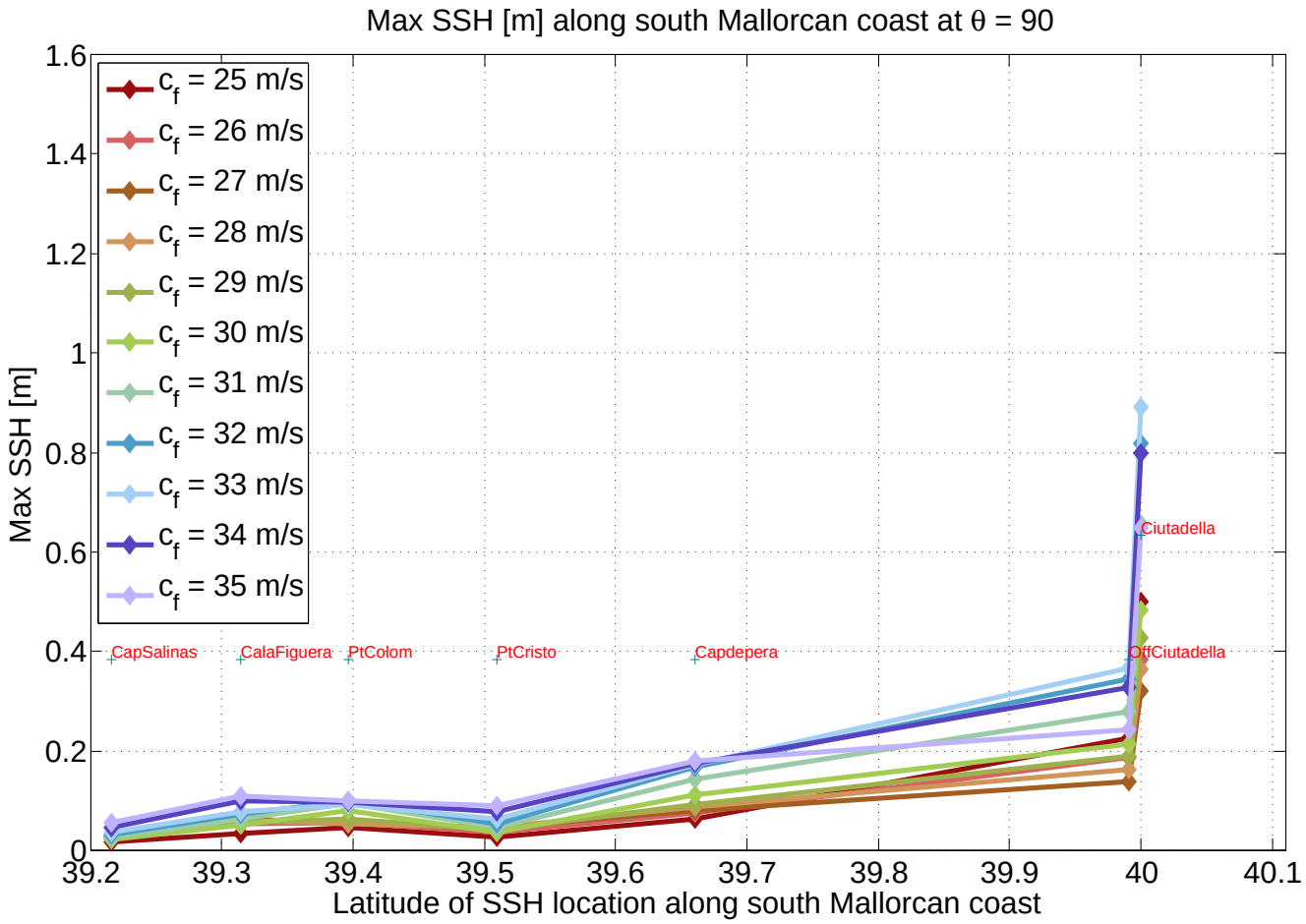


FIGURE 19: Maximum elevation developed along the east Mallorca shelf, depending on the the phase speed of the pressure disturbance and on the sampling location. The names of locations (red letters) are inserted at their respective latitudes for orientation.